Stem Cell Reports
Article

OPEN ACCESS

A Common Origin for B-1a and B-2 Lymphocytes in Clonal Pre- Hematopoietic Stem Cells

Brandon K. Hadland,[1,2,*] Barbara Varnum-Finney,[1] Pankaj K. Mandal,[3,4] Derrick J. Rossi,[3,4] Michael G. Poulos,[5,6] Jason M. Butler,[5,6] Shahin Rafii,[5] Mervin C. Yoder,[7] Momoko Yoshimoto,[7,8] and Irwin D. Bernstein[1,2]

[1]Clinical Research Division, Fred Hutchinson Cancer Research Center, 1100 Fairview Avenue N, D2-373, Seattle, WA 98109, USA
[2]Department of Pediatrics, University of Washington School of Medicine, Seattle, WA 98105, USA
[3]Department of Stem Cell and Regenerative Biology, Harvard University, Cambridge, MA 02138, USA
[4]Division of Hematology/Oncology, Program in Cellular and Molecular Medicine, Boston Children's Hospital, Boston, MA 02116, USA
[5]Department of Medicine, Ansary Stem Cell Institute
[6]Department of Surgery
Weill Cornell Medical College, New York, NY 10021, USA
[7]Department of Pediatrics, Herman B. Wells Center for Pediatric Research, Indiana University School of Medicine, Indianapolis, IN 46202, USA
[8]Present address: Center for Stem Cell and Regenerative Medicine, Brown Foundation Institute of Molecular Medicine, University of Texas Health Science Center at Houston, Houston, TX 77030, USA
*Correspondence: bhadland@fredhutch.org
http://dx.doi.org/10.1016/j.stemcr.2017.04.007

SUMMARY

Recent evidence points to the embryonic emergence of some tissue-resident innate immune cells, such as B-1a lymphocytes, prior to and independently of hematopoietic stem cells (HSCs). However, whether the full hematopoietic repertoire of embryonic HSCs initially includes these unique lineages of innate immune cells has been difficult to assess due to lack of clonal assays that identify and assess HSC precursor (pre-HSC) potential. Here, by combining index sorting of single embryonic hemogenic precursors with in vitro HSC maturation and transplantation assays, we analyze emerging pre-HSCs at the single-cell level, revealing their unique stage-specific properties and clonal lineage potential. Remarkably, clonal pre-HSCs detected between E9.5 and E11.5 contribute to the complete B cell repertoire, including B-1a lymphocytes, revealing a previously unappreciated common precursor for all B cell lineages at the pre-HSC stage and a second embryonic origin for B-1a lymphocytes.

INTRODUCTION

During embryonic development, hematopoietic cells arise from transient endothelial-like precursors known as hemogenic endothelium (HE), which are found initially in the yolk sac vascular plexus and later in various intraembryonic and extraembryonic vessels (Frame et al., 2016; Gordon-Keylock et al., 2013; Yzaguirre and Speck, 2016). An expanding number of studies have revealed multiple overlapping waves of hematopoietic progenitors generated from HE, which give rise to increasingly diverse hematopoietic lineages, including progenitors with erythroid, myeloid, and lymphoid potential detected prior to and independently of hematopoietic stem cells (HSCs) (Frame et al., 2013; Hadland et al., 2004; Kobayashi et al., 2014; Lin et al., 2014; Yoshimoto, 2015; Yoshimoto et al., 2012). Our group previously identified B-restricted progenitors that arise prior to HSCs with distinct B cell potential that includes B-1a cells, a lineage of tissue-resident B cells implicated in innate immune responses and autoimmunity (Yoshimoto et al., 2011). Further, mature B-1a cells are serially transplantable, suggesting an embryonic origin for life-long B-1a cells independent of HSCs and conventional (B-2) B cells (Kobayashi et al., 2014). Separate studies demonstrated that highly purified long-term HSCs from the adult bone marrow, transplanted to adult recipients, do not contribute significantly to the B-1a subset of B lymphocytes (Ghosn et al., 2012), further supporting the concept of a separate embryonic origin of the innate B-1a lineage. However, a recent study in which HSCs were defined functionally by long-term contribution to multilineage hematopoiesis using cellular barcoding techniques indicated contribution to both B-2 and B-1a cells by clonal fetal stage HSCs, whereas two separate studies examining whether highly purified fetal liver HSCs contribute to B-1a cells following transplantation produced conflicting results, potentially related to differences in phenotypic markers used for sorting HSCs from the fetal liver (Ghosn et al., 2016; Kristiansen et al., 2016). These studies suggest the possibility of heterogeneity within the fetal HSC pool with regard to B-1a potential and the need to determine the existence of a common precursor for HSCs and B-1a cells during early HSC development.

One of the significant challenges in understanding embryonic HSC development has been the lack of methods to distinguish clonal precursors of HSCs from temporally and phenotypically overlapping progenitors lacking HSC potential, which is necessary to identify the unique properties and lineage potential of emerging HSCs at the single-cell level. We previously described the generation of an

This is an open access article under the CC BY-NC-ND license (http://creativecommons.org/licenses/by-nc-nd/4.0/).

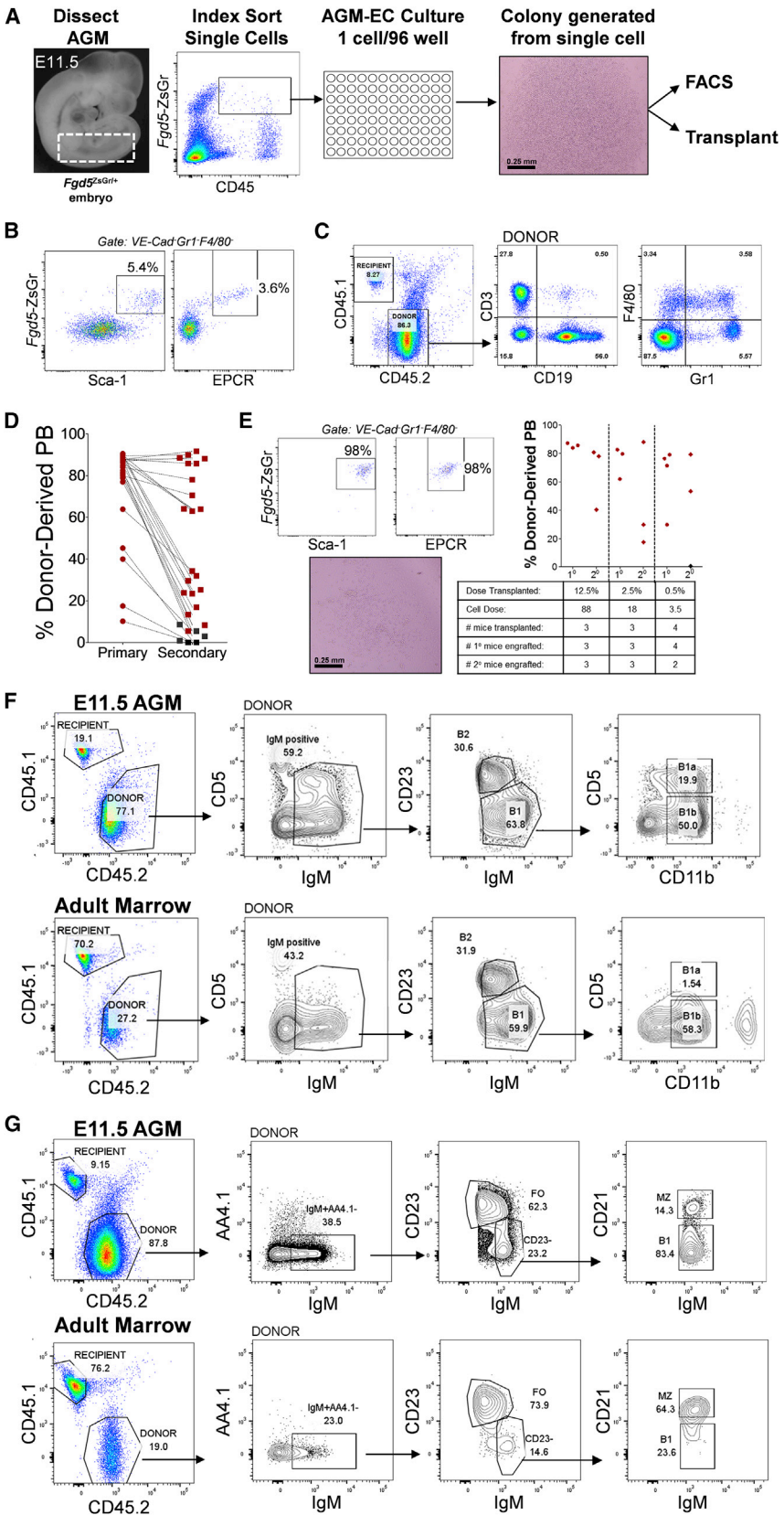

Figure 1. Index Sorting with AGM-EC Co-culture Identifies Clonal *Fgd5*-ZsGr^{+} CD45$^{+/lo}$ Pre-HSC with B-1a and B-2 Cell Potential

(A) Methodology for detection of clonal HSC precursors from E11.5 *Fgd5*$^{ZsGr/+}$ embryos combining index sorting of single AGM-derived cells and AGM-EC co-culture. Dashed box indicates sample window used for index sorting *Fgd5*-ZsGr^{+}CD45$^{+/lo}$ cells.

(B) Phenotypic analysis by FACS of the progeny of a single cell following 5 days co-culture, showing a population of cells co-expressing HSC markers *Fgd5*-ZsGr, Sca-1, and EPCR in cells gated as VE-Cadherin^{-} Gr1^{-}F4/80^{-}.

(C) Representative peripheral blood engraftment in a recipient mouse transplanted with the progeny of a single cell with the "HSC" phenotype as shown in (B)

(D) Primary and secondary peripheral blood engraftment from E11.5 pre-HSC clones (primary engraftment data at 12–16 weeks post-transplant, secondary engraftment at >16 weeks post-transplant, from n = 27 clones pooled from two independent experiments; clonal HSC precursor frequency 27 of 564 total index-sorted cells). Mice with multilineage engraftment are indicated by data points in red. Mice lacking detectable peripheral blood engraftment in one or more lineages are indicated by data points in black.

(E) Representative E11.5 pre-HSC clone generating a colony of progeny with homogeneous VE-Cadherin^{-}Gr1^{-}F4/80^{-}*Fgd5*-ZsGr^{+}Sca1^{+}EPCR^{+} "HSC" phenotype, with limit dilution transplantation of the progeny demonstrating primary (1°) and secondary (2°) engraftment. HSC frequency of the progeny calculated by limiting dilution analysis based on the fraction of mice with secondary engraftment (ELDA analysis; Hu and Smyth, 2009) is estimated at 1 in 4.5 cells (95% CI, 1 in 1.4 to 1 in 14), and total of 156 HSCs generated (95% CI, 50 to 486). Mice with multilineage engraftment at 12 weeks post-transplant in primary and16 weeks post-transplant in secondary transplants are indicated by data points in red.

(F and G) Representative engraftment of (F) B-1a, B-1b and B-2 cells in the peritoneum, and (G) B1, marginal zone (MZ), and follicular (FO) B cells in the spleen, 12 weeks following transplantation of the progeny (after AGM-EC co-culture) of

(legend continued on next page)

endothelial cell (EC) niche that supports HSC development from hemogenic precursors in vitro (Hadland et al., 2015). This EC niche is derived from the embryonic aorta-gonad-mesonephros region (AGM-EC), where the first adult-engrafting HSCs are detected during development. Specifically, we showed that co-culture with AGM-ECs was sufficient to support the induction of embryonic HE and pre-HSCs isolated as early as E9.5 to bona fide HSCs, as defined by their ability to provide long-term, multilineage engraftment into adult recipients. To build upon these studies and begin to identify the unique properties and lineage potential of clonal HSC precursors, we have adapted this system to analyze the potential of individual index-sorted hemogenic precursors to give rise to hematopoietic progeny, including functional HSCs following AGM-EC co-culture. Index sorting allows the correlation of the functional output of each single-sorted cell to its precise phenotypic properties collected during fluorescence-activated cell sorting (FACS), including the distinct expression intensity of each cell surface marker included for staining (Schulte et al., 2015). By this approach, here, we identify clonal precursors from the murine embryonic para-aortic splanchnopleura (P-Sp)/AGM region from E9.5 to E11.5 capable of giving rise to multilineage-engrafting HSCs, elucidating their unique phenotypic properties and demonstrating a common capacity to contribute to all B cell lineages including B-1a cells. Importantly, these studies provide a platform for further investigation of HSC precursors at single-cell resolution during their emergence and transition to HSCs, which will provide critical insight toward the future de novo engineering of HSCs for therapeutic applications.

RESULTS

Index Sorting Resolves Clonal E11.5 Pre-HSCs with Both B-1a and B-2 Cell Lineage Potential

To facilitate screening for HSC potential following AGM-EC co-culture, we employed a transgenic mouse expressing Zs-Green (ZsGr) in the *Fgd5* locus, which was reported to enable identification and purification of adult marrow HSCs, but also marked endothelial cells (Gazit et al., 2014). In the embryonic P-Sp/AGM, *Fgd5*-ZsGr expression is sensitive for, but not specific to, HSC precursors as it is expressed in all VE-Cadherin$^+$ cells (Figure S1A), which includes hemogenic precursors as well as non-hemogenic endothelial cells at this stage. Following AGM-EC co-culture of AGM-derived *Fgd5*-ZsGr$^+$VE-Cadherin$^+$ precursors cells, persistence of *Fgd5*-ZsGr expression in the VE-Cadherin$^-$F4/80$^-$Gr1$^-$ hematopoietic fraction distinguishes the population of hematopoietic cells with long-term multilineage primary and secondary engraftment potential (Figures S1B and S1C), thus making it useful in screening for generation of engrafting cells following co-culture of hemogenic precursors with AGM-ECs.

To characterize pre-HSCs from E11.5 AGM at the single-cell level, we index sorted single CD45$^{+/lo}$ZsGr$^+$ cells from dissected E11.5 *Fgd5*$^{+/ZsGr}$ AGM to individual wells of a 96-well plate containing an AGM-EC layer, and monitored for growth of hematopoietic colonies. Clonal frequency of colony formation ranged from 11% to 15% (n = 2). After 5 days of co-culture, cells from all wells, including those with and without hematopoietic colonies, were harvested (Figure 1A). Half of the cells from each well were assessed for expression of *Fgd5*-ZsGr and other phenotypic HSC markers, and half were transplanted to lethally irradiated adult Ly5.1 (CD45.1) congenic C57Bl6 wild-type mice along with 5 × 10^4 Ly5.1 rescue whole bone marrow cells to determine multilineage engraftment potential. By this approach, we found most hematopoietic colonies containing cells with VE-Cadherin$^-$Gr1$^-$F4/80$^-$Sca1$^+$EPCR$^+$*Fgd5*-ZsGr$^+$ phenotype (Figure 1B) were capable of long-term multilineage engraftment determined by detection of donor-lineage-positive cells in the peripheral blood (Figure 1C) of transplanted mice, and by detection of *Fgd5*-ZsGr$^+$ donor cells with HSC phenotype (Lineage$^-$ c-kit$^+$Sca-1$^+$CD48$^-$CD150$^+$) in the bone marrow (Figure S1D). In contrast, neither harvested hematopoietic colonies without detectable VE-Cadherin$^-$Gr1$^-$F4/80$^-$Sca1$^+$ EPCR$^+$*Fgd5*-ZsGr$^+$ cells nor cells harvested from wells without hematopoietic colonies provided detectable engraftment in transplanted mice (data not shown). In addition to assessing HSC potential following primary transplantation, we also examined secondary engraftment from individual pre-HSC clones. Most clonal E11.5 precursors capable of primary multilineage engraftment also provided multilineage secondary engraftment; however, a subset did not, suggesting heterogeneity in the ability of clonal pre-HSCs to give rise to HSCs with robust serial transplantation capacity (Figure 1D). Among engrafting pre-HSC clones, we also detected heterogeneity in colony phenotype (compare Figures 1B and 1E) and the extent of transplantation capacity. Specifically, we detected a subset of pre-HSCs that manifested extensive self-renewal behavior, generating large numbers of homogeneous

clonal E11.5 AGM-derived *Fgd5*-ZsGr$^+$CD45$^+$ pre-HSCs, or adult bone marrow-derived *Fgd5*-ZsGr$^+$Lin$^-$Sca1$^+$c-kit$^+$CD150$^+$CD48$^-$ HSCs. Similar results, demonstrating both B-1a and B-2 peritoneal engraftment, were obtained in all clones analyzed from E11.5 pre-HSCs (n = 27).
See Table S1.

phenotypic and functional HSCs with robust primary and secondary multilineage engraftment (Figure 1E), comparable with the proliferative behavior of fetal liver-stage HSCs, which eventually contribute to the more quiescent adult HSC pool (Bowie et al., 2007).

Considering recent studies suggesting potential heterogeneity in B-1a potential of fetal liver HSCs, single-cell analysis of embryonic HSC precursors also presented the unique opportunity to evaluate clonal contribution to B-1a B cell potential from developing HSCs prior to the fetal liver stage. Thus, we examined whether E11.5 pre-HSCs, which we have shown contribute clonally to long-term multilineage hematopoiesis in the peripheral blood and marrow following AGM-EC maturation and transplantation, also contribute to tissue-resident B-1a cells in the peritoneum. We found that all clonal pre-HSCs analyzed at E11.5 contributed to the complete B cell repertoire, including B-1a, B-1b, and B-2 cells in the peritoneum (Figures 1F and Table S1), and B1, marginal zone, and follicular (B-2) B cells in the spleen (Figure 1G). To rule out the possibility that co-culture on AGM-EC stroma induced B-1a potential in cells that otherwise lacked this potential, we also tested clonal adult bone marrow-derived *Fgd5*-ZsGr$^+$Lin$^-$Sca1$^+$c-kit$^+$CD48$^-$CD150$^+$ HSCs cultured on AGM-ECs. Consistent with previous studies in which purified adult HSCs were directly transplanted (Ghosn et al., 2012), the progeny of adult HSCs cultured on AGM-ECs contributed to multilineage hematopoiesis, including marginal zone, B-2, and B-1b B cells, but did not significantly contribute to the B-1a lineage detected in the peritoneum of transplanted mice (Figures 1F and 1G). Combined with our previous studies demonstrating an HSC-independent source of B-1a cells from early E9 yolk sac and P-Sp HE (Yoshimoto et al., 2011; Kobayashi et al., 2014), these results confirm a second origin of innate B-1a cells from clonal E11.5 AGM-derived pre-HSCs that is unique to embryonic development.

Functionally Distinct E9.5 Pre-HSCs Contain B-1a and B-2 Cell Lineage Potential

At E9.5, P-Sp cells co-expressing endothelial markers and CD41, the earliest marker of hematopoietic commitment expressed prior to CD45, represent a heterogeneous mixture of hematopoietic progenitors, including a rare population of pre-HSCs (1–2 per embryo) as determined by limiting dilution re-aggregation assays (Rybtsov et al., 2014, 2016). To determine whether we could identify these early pre-HSCs at the single-cell level, individual cells from E9.5 *Fgd5*$^{+/ZsGr}$ embryo P-Sp were index sorted based on CD41 and Zs-Green expression to AGM-ECs in 96-well plates and monitored for growth of hematopoietic colonies (Figure 2A). Clonal frequency of colony formation ranged from 8% to 27% (18% ± 8%, n = 4). *Fgd5*-ZsGr$^+$CD41^{lo} cells giving rise to colonies with phenotypic VE-Cadherin$^-$Gr1$^-$F4/80$^-$Sca1$^+$EPCR$^+$*Fgd5*-ZsGr$^+$ cells and long-term multilineage engraftment were identified, confirming a clonal origin for HSC precursors from this earlier population (Figures 2B and 2C). Compared with pre-HSC clones identified at E11.5, clonal *Fgd5*-ZsGr$^+$CD41^{lo} pre-HSCs detected at E9.5 were rare (less than 1 per embryo equivalent), contributed less robustly to multilineage hematopoiesis in secondary transplantation assays (Figure 2D), and did not generate any homogeneous (extensively self-renewing) HSC colonies that were observed from E11.5 pre-HSC clones, suggesting distinct properties of pre-HSC clones arising during this early stage of development compared with later pre-HSCs detected at E11.5. We also examined whether E9.5 pre-HSCs contribute to B-1a cells. Like pre-HSCs at E11.5, clonal pre-HSCs analyzed from E9.5 contributed to all B cell subsets examined, including B-1a, B-1b, and B-2 cells in the peritoneum (Figures 2E and Table S1), and B1, marginal zone, and follicular (B-2) B cells in the spleen (Figure 2F). Interestingly, the relative contribution of pre-HSCs is significantly skewed toward B-1a cells from E9.5 clones and toward B-2 cells from E11.5 clones (Table S1), providing further evidence for evolution of distinct, stage-dependent properties of pre-HSCs between E9.5 and E11.5.

Clonal Pre-HSC Are Distinguished by Unique Expression of EPCR and Dll4

If pre-HSCs constitute a distinct population among a larger population of hemogenic precursors lacking HSC potential, we hypothesized they may be distinguished by the expression of unique surface markers. Index sorting facilitates the determination of phenotypic characteristics of different hemogenic populations either with or without HSC potential, by tracking the phenotypic parameters of each individual cell as it correlates to its hematopoietic potential and engraftment potential following induction on AGM-EC stroma. Thus, we screened for additional surface markers that could further enrich for pre-HSCs. At E11.5, we determined that the subset of *Fgd5*-ZsGr$^+$CD45$^{+/lo}$ cells expressing high levels of EPCR, a marker previously shown to be expressed in fetal and adult long-term HSCs as well as embryonic pre-HSCs and multipotent progenitors (Balazs et al., 2006; Inlay et al., 2014; Iwasaki et al., 2010; Zhou et al., 2016), was significantly enriched in HSC potential, identifying a distinct phenotypic population with HSC potential at approximately 1 in 2 to 1 in 3 cells sorted (Figures 3A and S2A). Clonal pre-HSCs between E9.5 and E10.5 also express EPCR, although they remain significantly outnumbered by hemogenic precursors without HSC potential that are also detected in the *Fgd5*-ZsGr$^+$CD41^{lo}EPCR$^+$ population at these earlier stages; however, expression of the Notch ligand Dll4, a marker of arterial endothelium, distinguishes pre-HSCs at these stages since

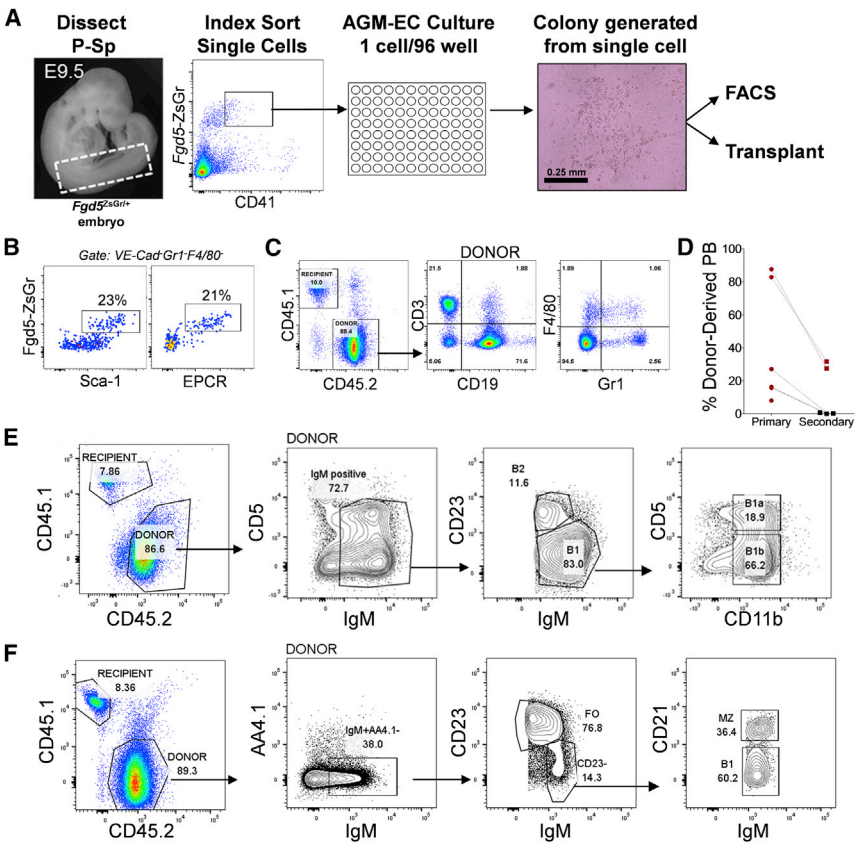

Figure 2. Clonal *Fgd5*-ZsGr^{+}CD41^{lo} E9.5 Pre-HSC Have B-1a and B-2 Cell Potential

(A) Methodology for detection of clonal HSC precursors from E9.5 *Fgd5*$^{ZsGr/+}$ embryos combining index sorting of single P-Sp-derived cells and AGM-EC co-culture. Dashed box indicates sample window used for index sorting *Fgd5*-ZsGr^{+}CD41^{lo} cells.

(B) Phenotypic analysis by FACS of progeny of a single cell following 7 day co-culture, showing a population of cells co-expressing HSC markers *Fgd5*-ZsGr, Sca-1, and EPCR in cells gated as VE-Cadherin^{-}Gr1^{-}F4/80^{-}.

(C) Representative peripheral blood engraftment in a mouse transplanted with progeny of a single cell with "HSC" phenotype as shown in (B).

(D) Primary and secondary peripheral blood engraftment from E9.5 pre-HSC clones (primary engraftment data from n = 6 clones at 12–16 weeks post-transplant, secondary engraftment data from n = 5 clones at >16 weeks post-transplant, pooled from four independent experiments; clonal HSC precursor frequency 6 of 653 total index sorted cells). Mice with multilineage engraftment are indicated by data points in red. Mice lacking detectable peripheral blood engraftment in one or more lineages are indicated by data points in black.

(E and F) Representative engraftment of (E) B-1a, B-1b, and B-2 cells in the peritoneum, and (F) B1, marginal zone (MZ), and follicular (FO) B cells in the spleen, 12 weeks following transplantation of the progeny (after AGM-EC co-culture) of clonal E9.5 P-Sp-derived *Fgd5*-ZsGr^{+}CD41^{lo} pre-HSCs. Similar results, demonstrating both B-1a and B-2 peritoneal engraftment, were obtained in all clones analyzed from E9.5 pre-HSCs (n = 6).

See Table S1.

most EPCR^{+} precursors lacking HSC potential express lower levels of Dll4 (Figures 3B, S2B, and S2C). We confirmed that Dll4 expression also enriched for HSC potential at the population level in both VE-Cadherin^{+}CD41^{-}CD45^{-} HE as well as VE-Cadherin^{+}CD41^{+}/CD45^{+} hematopoietic populations from E9.5 P-Sp, by sorting these populations based on Dll4 expression followed by AGM-EC co-culture and transplantation into adult mice (Figure 3C). These results demonstrate the ability to resolve distinct phenotypic populations of hemogenic precursors capable of generating HSCs from those that cannot, which favors the existence of unique populations of precursors at this stage with and without HSC potential, rather than simply reflecting inefficiencies of the co-culture assay.

DISCUSSION

To establish methods for the study of the functional and molecular properties of HSC precursors at the single-cell level, we have adapted our recently described 2D co-culture system, in which an engineered AGM-derived EC substrate provides the necessary in vitro niche for induction of functional HSCs from hemogenic precursors (Hadland et al., 2015), for clonal studies of index-sorted hemogenic precursors from embryonic development. By this approach, we have demonstrated that functionally defined, clonal pre-HSCs are phenotypically distinguishable from progenitors lacking HSC potential in the E9.5 to E11.5 embryo. Interestingly, we identified Dll4, a Notch ligand expressed on arterial endothelium, as a phenotypic marker of HSC precursor potential. Considering recent studies suggesting that the level of Notch signaling activation must be attenuated during the HE to HSC transition, it is interesting to speculate that co-expression of Dll4 with Notch1 on the surface of an HSC precursor could serve to limit Notch1 receptor activation by *cis*-inhibition, a well-established mechanism regulating Notch signaling in other development systems (del Álamo et al., 2011; Gama-Norton et al., 2015; Lizama et al., 2015). This could constitute a

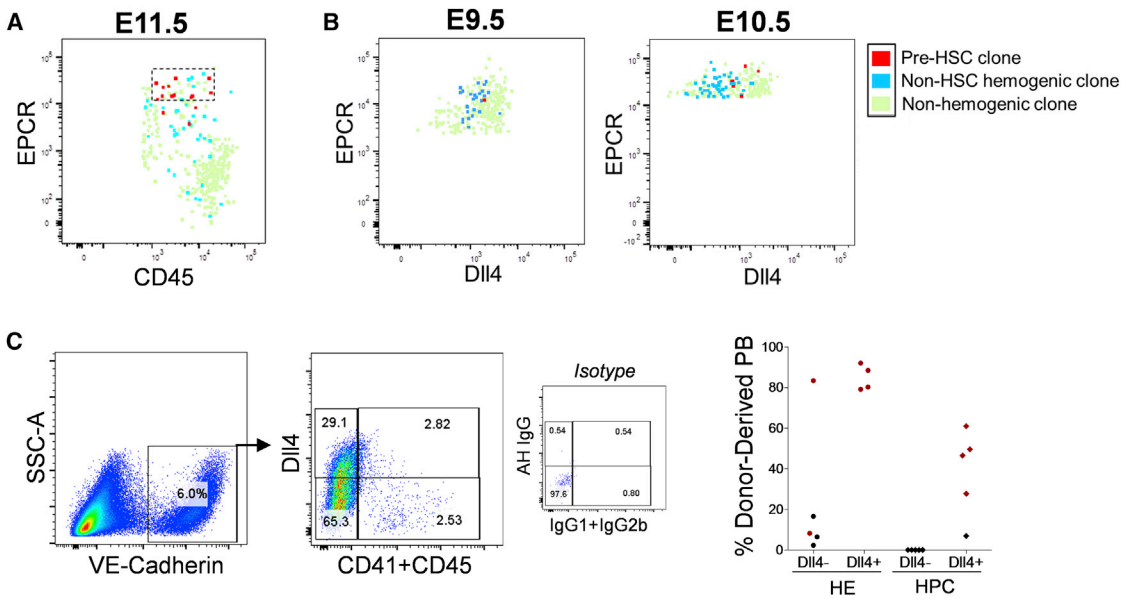

Figure 3. Pre-HSCs Express Distinct Levels of EPCR and Delta-like-4

(A) Expression of EPCR in index-sorted E11.5 AGM-derived *Fgd5*-ZsGr^{+}CD45$^{+/lo}$ single cells, identifying precursors with HSC potential (pre-HSC clone), hematopoietic colony formation without HSC potential (non-HSC hemogenic clone), or no hematopoietic colony formation (non-hemogenic clone) based on functional potential following AGM-EC co-culture. Dashed box contains EPCR^{high}-expressing cells highly enriched for pre-HSC clones.

(B) Expression of EPCR and Delta-like-4 (Dll4) in index-sorted E9.5 (left panel) and E10.5 (right panel) P-Sp/AGM-derived *Fgd5*-ZsGr^{+}CD41^{lo} single cells (see also Figure S2 for additional index-sorting parameters).

(C) Engraftment of hematopoietic cells generated following co-culture on AGM-ECs from E9.5 P-Sp hemogenic endothelium (HE, VE-Cadherin^{+}CD41^{-}CD45^{-}) and hematopoietic progenitor cells (HPC, VE-Cadherin^{+}CD41^{+} and/or CD45^{+}) sorted based on expression of Dll4. Mice with multilineage engraftment at >16 weeks post-transplant are indicated by red data points. Mice lacking detectable peripheral blood engraftment in one or more lineages are indicated by data points in black.

cell-autonomous mechanism to modulate the ability of pre-HSCs to receive Notch signals induced by *trans* activation via Notch ligands known to be expressed on adjacent endothelial cell stroma (Hadland et al., 2015), which may be essential for HSC fate, as studies including our own have demonstrated that fate determination in many developmental contexts is dependent on precise Notch signal strength (Dallas et al., 2005; Delaney et al., 2005). Additional studies will be necessary to determine the functional significance of Dll4 expression on HSC precursors in this regard, studies that may provide insight into requirements for generation of functional HSC from pluripotent stem cell-derived hemogenic precursors.

Our current study also enabled the assessment of clonal contribution to in vivo multilineage hematopoiesis from single cells at the earliest stages of HSC precursor formation, which has allowed us to identify the earliest common precursor of B-1a and B-2 cell potential in a clonal precursor to HSCs as early as E9.5. Recent reports have strengthened the concept that adult HSCs do not contribute significantly to the innate B-1a cell compartment, but suggest heterogeneity in the fetal HSC compartment with regard to B-1a cell potential (Beaudin et al., 2016; Ghosn et al., 2012, 2016; Kristiansen et al., 2016; Sawai et al., 2016). Previous studies by members of our group identified an embryonic HSC-independent B cell progenitor with B-1 but not B-2 cell potential (Kobayashi et al., 2014; Yoshimoto, 2015; Yoshimoto et al., 2011). Our ability to detect significant B-1a and B-2 cell contribution from all clonal pre-HSC tested at E9.5 and E11.5 in this study suggests a second wave of B-1a progenitors developing from a common precursor to embryonic HSCs.

A recently published study using an irreversible lineage reporter mouse model identified two distinct populations of fetal liver HSCs (Beaudin et al., 2016). Although both types provide long-term multilineage engraftment in transplantation assays, only one of these fetal HSC populations contributes to the pool of long-term HSCs in the adult bone marrow in situ, whereas the other "developmentally restricted" HSC is primed to contribute to innate immune cells, including the B-1a lineage. Our clonal analysis of emerging pre-HSCs suggests

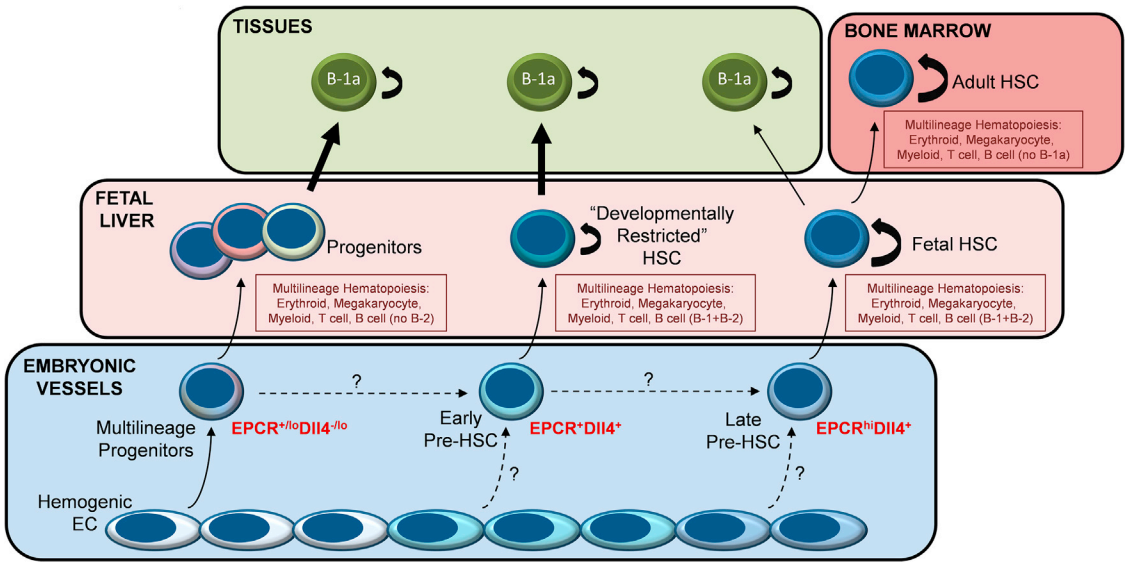

Figure 4. Proposed Model for Multiple Waves of Definitive Hematopoiesis Contributing to B-1a B Cells

Multiple overlapping waves of definitive hematopoiesis emerge within embryonic vessels between E9 and E11.5, giving rise initially to multilineage progenitors producing erythroid, myeloid, and innate-immune lymphoid progeny independently of HSC (Böiers et al., 2013; Godin et al., 1993; Inlay et al., 2014; Kobayashi et al., 2014; Yoshimoto et al., 2011; Yoshimoto et al., 2012), followed by emergence of the earliest clonal pre-HSCs giving rise to "developmentally restricted" HSCs with innate-immune biased lymphoid potential (Beaudin et al., 2016), and late pre-HSC clones giving rise to a pool of extensively self-renewing fetal liver HSCs that initially have limited B-1a B cell potential, which is lost as they establish the life-long HSC pool of the adult bone marrow (Ghosn et al., 2012).

developmental asynchrony, with E9.5 pre-HSCs generating a relatively greater proportion of B-1a cells in transplantation assays and unique pre-HSC clones emerging only later at E11.5 with extensive expansion in vitro of HSCs with robust primary and secondary engraftment, consistent with the self-renewing behavior of expanding fetal liver HSCs that populate the adult marrow (Bowie et al., 2007). These results suggest that pre-HSCs, arising asynchronously between E9.5 and E11.5, generate HSCs with different functional properties and relative B-1a cell contribution that may account for the distinct populations of fetal liver HSCs described by Beaudin et al. (2016).

Altogether, combining the results of these recent studies with our clonal analysis of pre-HSC lineage potential presented here, we propose a refined model of developmental hematopoiesis that incorporates multiple, overlapping waves of definitive hematopoiesis, progressing through a multilineage progenitor stage generating innate immune cells including B-1a but lacking B-2 potential, early pre-HSCs giving rise to "developmentally restricted" HSCs that are biased toward generation of innate immune cells including B-1a but also generate initial B-2 cells, and late pre-HSCs with limited B-1a potential that is lost as these cells mature, self-renew, and contribute to the rapidly expanding pool of long-term fetal liver HSCs that eventually colonize the adult marrow (Figure 4). Consistent with a recently reported genetic study proposing distinct, differentially regulated waves of B-1a and B-2 cell development, this model accounts for three distinct sources of B-1a and two sources of B-2 cell potential (Montecino-Rodriguez et al., 2016). Future studies using our approach to define HSC potential at the clonal level will be required to determine whether these distinct waves of definitive hematopoiesis emerge from separate populations of HE or rather diverge following emergence of a common pool of $CD41^{+}$ hematopoietic precursors. Altogether, our studies provide insight into the developmental origin of HSC heterogeneity, with critical implications for engineering HSCs from pluripotent stem cells and for understanding the ontogeny of innate immunity.

EXPERIMENTAL PROCEDURES

Mice

Wild-type C57BL6/J7 (Ly5.2/CD45.2) and congenic C57BL/6.SJL-Ly5.1-Pep3b (Ly5.1/CD45.1) mice were bred at the Fred Hutchinson Cancer Research Center. Transgenic *Fgd5*$^{Zs\text{-}Green/+}$ mice in C57BL6/J7 background were generated as previously described (Gazit et al., 2014). C57BL6/J7 Ly5.2 or *Fgd5*$^{Zs\text{-}Green/+}$ male and wild-type C57BL6/J7 Ly5.2 female mice were used for timed matings.

Embryo Dissections and Cell Sorting

Embryo P-Sp/AGM tissues were harvested as previously described (Hadland et al., 2015). Embryo age was precisely timed by counting somite pairs (sp): E9.5 (21–29sp), E10.5 (35–39sp), and E11.5 (40–47sp). Dissected AGM/P-Sp tissues were treated with 0.25% collagenase (STEMCELL Technologies) for 25 min at 37°C, pipetted to a single-cell suspension, and washed with PBS containing 10% fetal bovine serum (FBS). Cells were incubated with anti-mouse CD16/CD32 (FcγRII block) and stained with monoclonal antibodies as indicated. A detailed list of all antibodies used is shown in Table S2. DAPI staining was used to gate out dead cells. All reagents for cell staining were diluted in PBS with 10% FBS, and staining was carried out on ice or at 4°C. Cells were sorted on a BD FACSAria II equipped with BD FACSDiva Software with index-sorting capability. For index-sorted single cells, sorting was performed in single-cell mode with maximum purity mask settings to minimize contaminating cells.

Endothelial Cell Co-culture Assays

AGM-ECs were derived from ECs sorted from E10.5 to E11.5 AGM regions, infected with lentivirus containing MyrAKT construct, and cultured as previously described (Hadland et al., 2015). For co-culture experiments, AGM-ECs at passage 15 or less were plated at a density of 1×10^4 cells per well to gelatin-treated 96-well tissue culture plates for single-cell assays, or 4×10^4 cells per 24-well for bulk cultures, 24 hr prior to initiation of co-culture. Single P-Sp/AGM-derived cells were individually index sorted to each well of 96-well plates containing AGM-ECs in serum-free media consisting of X-vivo 20 (Lonza) with recombinant cytokines (Peprotech): stem cell factor and FLT3 ligand each at 100 ng/mL, and interleukin-3, and thrombopoietin each at 20 ng/mL. Cells from E9.5 embryos were cultured for 7 days, and cells from E10.5 to 11.5 embryos were cultured for 5–6 days, based on prior studies that determined the time required to detect engrafting populations following culture from precursors at different stages (Hadland et al., 2015). Following co-culture, each well was visualized for hematopoietic colony formation, and wells with more than one colony were excluded from analysis. In some experiments, wells without visible hematopoietic colonies were also harvested for phenotypic and transplantation analysis to assay for HSC generation in the absence of colony formation.

Cell Surface Analysis

Following co-culture, 50% volume of each 96-well containing a visible colony was harvested by vigorous pipetting from the EC layer and transferred to new 96-well plates for FACS. Cells were spun and re-suspended in PBS with 2% FBS, pre-incubated with anti-mouse CD16/CD32 (FcγRII block) and then stained with various combinations of monoclonal antibodies as indicated. AGM-ECs were excluded from analysis of co-cultured cells by gating based on expression of VE-Cadherin, and myeloid cells were gated by expression of Gr-1 and F4/80. DAPI was used to exclude dead cells. Flow cytometry was performed on a Becton Dickinson Canto 2 and data analyzed using FlowJo Software.

Transplantation Assays

Freshly sorted Ly5.2/CD45.2 AGM cells or cultured cells harvested by pipetting off the wells were washed with PBS with 2% FBS and re-suspended in 100 μL of PBS/2% FBS per mouse transplanted. For clonal assays, the remaining 50% volume following FACS analysis of each 96-well plate containing a visible colony was harvested individually for transplantation. For most experiments, only colonies with detectable VE-Cadherin$^-$Gr1$^-$F4/80$^-$Sca1$^+$EPCR$^+$*Fgd5*-ZsGr$^+$ cells by FACS were transplanted based on initial studies demonstrating that colonies lacking this phenotype did not provide detectable hematopoietic engraftment in transplanted mice. Freshly harvested Ly5.1/CD45.1 bone marrow cells were added at 5×10^4 cells in 100 μL of PBS/FBS per mouse to provide hematopoietic rescue. Cells were co-injected into lethally irradiated (1,000 cGy using a cesium source) Ly5.1/CD45.1 adult recipients via the tail vein. For secondary transplants, 2×10^6 whole bone marrow cells harvested from primary recipients 12–16 weeks following primary transplantation were transplanted to lethally irradiated Ly5.1/CD45.1 recipients via the tail vein. FACS analysis of peripheral blood obtained by retro-orbital bleeds was performed at 2, 6, and 12–16 weeks following transplantation, and from cells obtained from harvested bone marrow, spleen, and thymic tissues, and peritoneal fluid at the time of secondary transplant, at 12–16 weeks following primary transplant. FACS analysis of peripheral blood was performed at 16 weeks following secondary transplantation. Peritoneal cells were harvested by injecting 6 mL of PBS with a 21G needle and syringe through the peritoneal membrane into the peritoneal space and collecting back injected fluid. Lineage-specific staining from donor (CD45.2) and recipient/rescue (CD45.1) cells for peripheral blood, bone marrow, spleen, thymus, and peritoneal-derived cells was performed as previously described (Hadland et al., 2015; Kobayashi et al., 2014), using antibodies listed in Table S2. Multilineage engraftment was defined as >5% donor (CD45.2) contribution to the peripheral blood with detectable contribution of donor myeloid (Gr-1 and/or F4/80), B cells (CD19), and T cells (CD3).

Statistics

For statistical analysis, two-tailed, unpaired Student's t test was used to calculate p values. A p value less than 0.05 was considered significant. ELDA software (Hu and Smyth, 2009) (http://bioinf.wehi.edu.au/software/elda/) was used for limit dilution transplantation analysis, calculated using the fraction of mice engrafted at each dilution of starting cells expressed per embryo equivalent, where engraftment was defined as >5% donor (CD45.2) contribution to the peripheral blood with each of donor myeloid (Gr-1 and/or F4/80), B cell (CD19) and T cell (CD3) engraftment detected in secondarily transplanted mice at 16 weeks post-transplant.

Animal Study Approval

All animal studies were conducted in accordance with the NIH guidelines for humane treatment of animals and were approved by the Institutional Animal Care and Use Committee at the Fred Hutchinson Cancer Research Center.

SUPPLEMENTAL INFORMATION

Supplemental Information includes two figures and two tables and can be found with this article online at http://dx.doi.org/10.1016/j.stemcr.2017.04.007.

AUTHOR CONTRIBUTIONS

B.K.H., B.V., I.D.B., S.R, J.M.B., M.G.P., M.C.Y., and M.Y. designed experiments. B.K.H., B.V., and M.Y. conducted experiments. P.K.M. and D.J.R. provided *Fgd5*$^{Zs\text{-}Green/+}$ mice. B.K.H. and B.V. wrote the manuscript and I.B., M.C.Y., P.K.M., D.J.R., and M.Y. edited the manuscript.

ACKNOWLEDGMENTS

We thank Cynthia McKay and David A. Flowers for their superb technical assistance. This work was supported by the NIH: NHLBI UO1 HL100395, Ancillary HL100395-07 Sub-award 10560, Ancillary HL099997, NIAID R56 AI110831, and NIAID R01 AI121197. Brandon Hadland is supported by the Alex's Lemonade Stand Foundation and Hyundai Hope on Wheels Foundation

Received: January 18, 2017
Revised: April 5, 2017
Accepted: April 6, 2017
Published: May 4, 2017

REFERENCES

Balazs, A.B., Fabian, A.J., Esmon, C.T., and Mulligan, R.C. (2006). Endothelial protein C receptor (CD201) explicitly identifies hematopoietic stem cells in murine bone marrow. Blood *107*, 2317–2321.

Beaudin, A.E., Boyer, S.W., Perez-Cunningham, J., Hernandez, G.E., Derderian, S.C., Jujjavarapu, C., Aaserude, E., MacKenzie, T., and Forsberg, E.C. (2016). A transient developmental hematopoietic stem cell gives rise to innate-like B and T cells. Cell Stem Cell *19*, 768–783.

Bowie, M.B., Kent, D.G., Dykstra, B., McKnight, K.D., McCaffrey, L., Hoodless, P.A., and Eaves, C.J. (2007). Identification of a new intrinsically timed developmental checkpoint that reprograms key hematopoietic stem cell properties. Proc. Natl. Acad. Sci. USA *104*, 5878–5882.

Böiers, C., Carrelha, J., Lutteropp, M., Luc, S., Green, J.C., Azzoni, E., Woll, P.S., Mead, A.J., Hultquist, A., Swiers, G., et al. (2013). Lymphomyeloid contribution of an immune-restricted progenitor emerging prior to definitive hematopoietic stem cells. Cell Stem Cell *13*, 535–548.

Dallas, M.H., Varnum-Finney, B., Delaney, C., Kato, K., and Bernstein, I.D. (2005). Density of the Notch ligand Delta1 determines generation of B and T cell precursors from hematopoietic stem cells. J. Exp. Med. *201*, 1361–1366.

del Álamo, D., Rouault, H., and Schweisguth, F. (2011). Mechanism and significance of cis-inhibition in Notch signalling. Curr. Biol. *21*, R40–R47.

Delaney, C., Varnum-Finney, B., Aoyama, K., Brashem-Stein, C., and Bernstein, I.D. (2005). Dose-dependent effects of the Notch ligand Delta1 on ex vivo differentiation and in vivo marrow repopulating ability of cord blood cells. Blood *106*, 2693–2699.

Frame, J.M., McGrath, K.E., and Palis, J. (2013). Erythro-myeloid progenitors: "definitive" hematopoiesis in the conceptus prior to the emergence of hematopoietic stem cells. Blood Cells Mol. Dis. *51*, 220–225.

Frame, J.M., Fegan, K.H., Conway, S.J., McGrath, K.E., and Palis, J. (2016). Definitive hematopoiesis in the yolk sac emerges from Wnt-responsive hemogenic endothelium independently of circulation and arterial identity. Stem Cells *34*, 431–444.

Gama-Norton, L., Ferrando, E., Ruiz-Herguido, C., Liu, Z., Guiu, J., Islam, A.B., Lee, S.U., Yan, M., Guidos, C.J., López-Bigas, N., et al. (2015). Notch signal strength controls cell fate in the haemogenic endothelium. Nat. Commun. *6*, 8510.

Gazit, R., Mandal, P.K., Ebina, W., Ben-Zvi, A., Nombela-Arrieta, C., Silberstein, L.E., and Rossi, D.J. (2014). Fgd5 identifies hematopoietic stem cells in the murine bone marrow. J. Exp. Med. *211*, 1315–1331.

Ghosn, E.E., Yamamoto, R., Hamanaka, S., Yang, Y., Herzenberg, L.A., and Nakauchi, H. (2012). Distinct B-cell lineage commitment distinguishes adult bone marrow hematopoietic stem cells. Proc. Natl. Acad. Sci. USA *109*, 5394–5398.

Ghosn, E.E., Waters, J., Phillips, M., Yamamoto, R., Long, B.R., Yang, Y., Gerstein, R., Stoddart, C.A., Nakauchi, H., and Herzenberg, L.A. (2016). Fetal hematopoietic stem cell transplantation fails to fully regenerate the B-lymphocyte compartment. Stem Cell Rep. *6*, 137–149.

Godin, I.E., Garcia-Porrero, J.A., Coutinho, A., Dieterlen-Lièvre, F., and Marcos, M.A. (1993). Para-aortic splanchnopleura from early mouse embryos contains B1a cell progenitors. Nature *364*, 67–70.

Gordon-Keylock, S., Sobiesiak, M., Rybtsov, S., Moore, K., and Medvinsky, A. (2013). Mouse extraembryonic arterial vessels harbor precursors capable of maturing into definitive HSCs. Blood *122*, 2338–2345.

Hadland, B.K., Huppert, S.S., Kanungo, J., Xue, Y., Jiang, R., Gridley, T., Conlon, R.A., Cheng, A.M., Kopan, R., and Longmore, G.D. (2004). A requirement for Notch1 distinguishes 2 phases of definitive hematopoiesis during development. Blood *104*, 3097–3105.

Hadland, B.K., Varnum-Finney, B., Poulos, M.G., Moon, R.T., Butler, J.M., Rafii, S., and Bernstein, I.D. (2015). Endothelium and NOTCH specify and amplify aorta-gonad-mesonephros-derived hematopoietic stem cells. J. Clin. Invest. *125*, 2032–2045.

Hu, Y., and Smyth, G.K. (2009). ELDA: extreme limiting dilution analysis for comparing depleted and enriched populations in stem cell and other assays. J. Immunol. Methods *347*, 70–78.

Inlay, M.A., Serwold, T., Mosley, A., Fathman, J.W., Dimov, I.K., Seita, J., and Weissman, I.L. (2014). Identification of multipotent progenitors that emerge prior to hematopoietic stem cells in embryonic development. Stem Cell Rep. *2*, 457–472.

Iwasaki, H., Arai, F., Kubota, Y., Dahl, M., and Suda, T. (2010). Endothelial protein C receptor-expressing hematopoietic stem cells reside in the perisinusoidal niche in fetal liver. Blood *116*, 544–553.

Kobayashi, M., Shelley, W.C., Seo, W., Vemula, S., Lin, Y., Liu, Y., Kapur, R., Taniuchi, I., and Yoshimoto, M. (2014). Functional B-1 progenitor cells are present in the hematopoietic stem cell-deficient embryo and depend on Cbfβ for their development. Proc. Natl. Acad. Sci. USA *111*, 12151–12156.

Kristiansen, T.A., Jaensson Gyllenbäck, E., Zriwil, A., Björklund, T., Daniel, J.A., Sitnicka, E., Soneji, S., Bryder, D., and Yuan, J. (2016). Cellular barcoding links B-1a B cell potential to a fetal hematopoietic stem cell state at the single-cell level. Immunity *45*, 346–357.

Lin, Y., Yoder, M.C., and Yoshimoto, M. (2014). Lymphoid progenitor emergence in the murine embryo and yolk sac precedes stem cell detection. Stem Cells Dev. *23*, 1168–1177.

Lizama, C.O., Hawkins, J.S., Schmitt, C.E., Bos, F.L., Zape, J.P., Cautivo, K.M., Borges Pinto, H., Rhyner, A.M., Yu, H., Donohoe, M.E., et al. (2015). Repression of arterial genes in hemogenic endothelium is sufficient for haematopoietic fate acquisition. Nat. Commun. *6*, 7739.

Montecino-Rodriguez, E., Fice, M., Casero, D., Berent-Maoz, B., Barber, C.L., and Dorshkind, K. (2016). Distinct genetic networks orchestrate the emergence of specific waves of fetal and adult B-1 and B-2 development. Immunity *45*, 527–539.

Rybtsov, S., Batsivari, A., Bilotkach, K., Paruzina, D., Senserrich, J., Nerushev, O., and Medvinsky, A. (2014). Tracing the origin of the HSC hierarchy reveals an SCF-dependent, IL-3-independent CD43(-) embryonic precursor. Stem Cell Rep. *3*, 489–501.

Rybtsov, S., Ivanovs, A., Zhao, S., and Medvinsky, A. (2016). Concealed expansion of immature precursors underpins acute burst of adult HSC activity in foetal liver. Development *143*, 1284–1289.

Sawai, C.M., Babovic, S., Upadhaya, S., Knapp, D.J., Lavin, Y., Lau, C.M., Goloborodko, A., Feng, J., Fujisaki, J., Ding, L., et al. (2016). Hematopoietic stem cells are the major source of multilineage hematopoiesis in adult animals. Immunity *45*, 597–609.

Schulte, R., Wilson, N.K., Prick, J.C., Cossetti, C., Maj, M.K., Gottgens, B., and Kent, D.G. (2015). Index sorting resolves heterogeneous murine hematopoietic stem cell populations. Exp. Hematol. *43*, 803–811.

Yoshimoto, M. (2015). The first wave of B lymphopoiesis develops independently of stem cells in the murine embryo. Ann. N. Y Acad. Sci. *1362*, 16–22.

Yoshimoto, M., Montecino-Rodriguez, E., Ferkowicz, M.J., Porayette, P., Shelley, W.C., Conway, S.J., Dorshkind, K., and Yoder, M.C. (2011). Embryonic day 9 yolk sac and intra-embryonic hemogenic endothelium independently generate a B-1 and marginal zone progenitor lacking B-2 potential. Proc. Natl. Acad. Sci. USA *108*, 1468–1473.

Yoshimoto, M., Porayette, P., Glosson, N.L., Conway, S.J., Carlesso, N., Cardoso, A.A., Kaplan, M.H., and Yoder, M.C. (2012). Autonomous murine T-cell progenitor production in the extra-embryonic yolk sac before HSC emergence. Blood *119*, 5706–5714.

Yzaguirre, A.D., and Speck, N.A. (2016). Insights into blood cell formation from hemogenic endothelium in lesser-known anatomic sites. Dev. Dyn. *245*, 1011–1028.

Zhou, F., Li, X., Wang, W., Zhu, P., Zhou, J., He, W., Ding, M., Xiong, F., Zheng, X., Li, Z., et al. (2016). Tracing haematopoietic stem cell formation at single-cell resolution. Nature *533*, 487–492.

Stem Cell Reports, Volume *8*

Supplemental Information

A Common Origin for B-1a and B-2 Lymphocytes in Clonal Pre- Hematopoietic Stem Cells

Brandon K. Hadland, Barbara Varnum-Finney, Pankaj K. Mandal, Derrick J. Rossi, Michael G. Poulos, Jason M. Butler, Shahin Rafii, Mervin C. Yoder, Momoko Yoshimoto, and Irwin D. Bernstein

SUPPLEMENTAL FIGURES

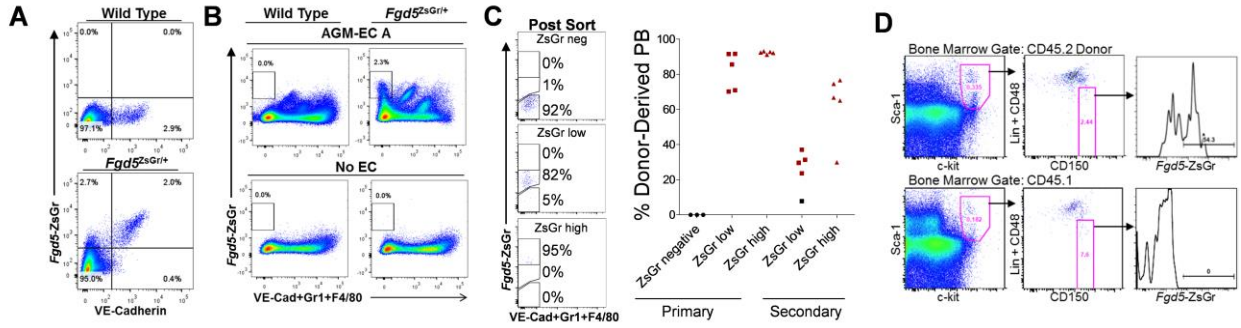

Figure S1. *Fgd5*-ZsGr expression tracks HSC potential following AGM-EC co-culture of VE-Cadherin^{+}CD45$^{+/lo}$ pre-HSC isolated from E11.5 *Fgd5*$^{ZsGr/+}$ embryo AGM, Related to Figures 1 and 2. A) Co-expression of *Fgd5*-ZsGr and VE-Cadherin in cells from dissected AGM regions of E11.5 *Fgd5*$^{ZsGr/+}$ embryos and wild type littermates. B) Expression of *Fgd5*-ZsGr in cells following 5 day culture of VE-Cadherin^{+}CD45$^{+/lo}$ pre-HSC from AGM regions of E11.5 *Fgd5*$^{ZsGr/+}$ embryos and wild type littermates with either AGM-EC or in the absence of EC stroma. Cells expressing VE-Cadherin, Gr1, or F4/80 are gated out to exclude autofluorescent myeloid and endothelial cells. C) Donor-derived peripheral blood engraftment in primary mice (at 24 weeks) and secondary mice (at 16 weeks) transplanted with cells sorted following 5 day culture of VE-Cadherin^{+}CD45$^{+/lo}$ pre-HSC from AGM regions of E11.5 *Fgd5*$^{ZsGr/+}$ embryos, based on expression of *Fgd5*-ZsGr expression (negative, low and high *Fgd5*-ZsGr expression, after gating out cells expressing VE-Cadherin, Gr1, or F4/80). D) Bone marrow engraftment from progeny of single cell (Figure 1B-C), demonstrating *Fgd5*-ZsGr expression in donor-derived (CD45.2) Lineage^{-}Sca1^{+}c-kit^{+}CD150^{+}CD48^{-} phenotypic HSC.

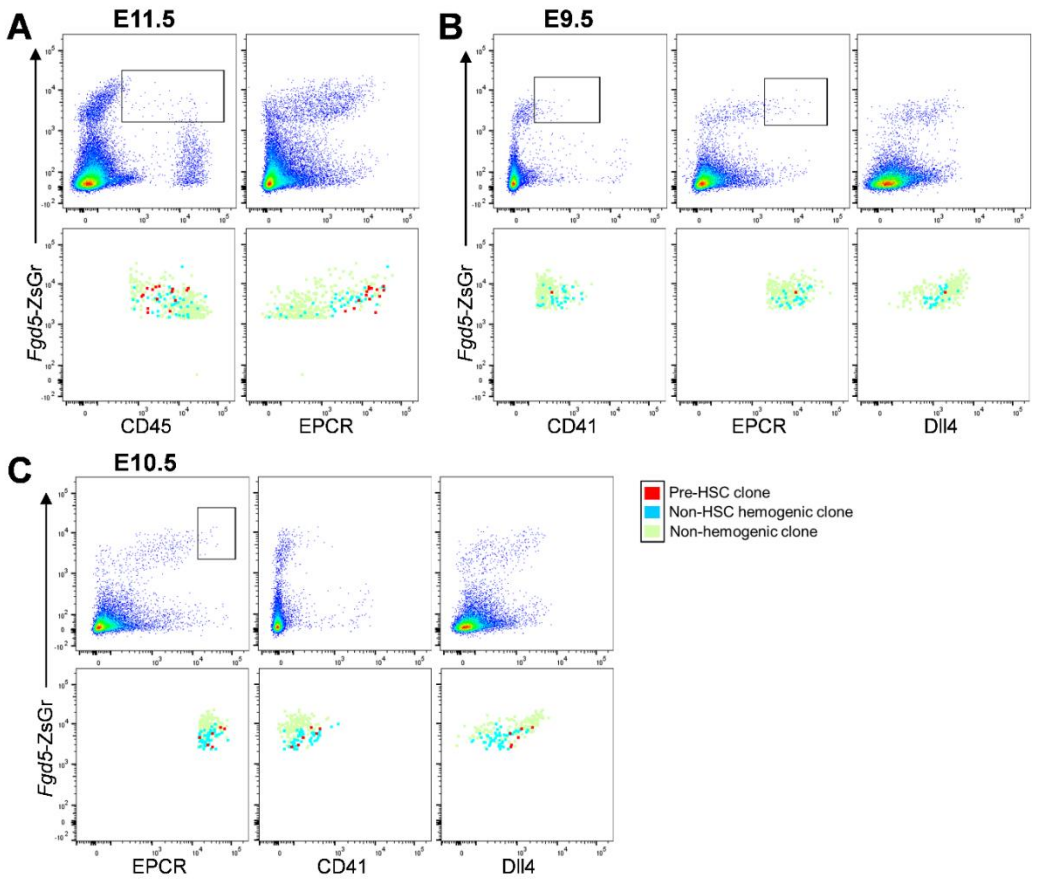

Figure S2. Index sorting parameters of functionally distinct hemogenic precursors, Related to Figure 3. Representative FACS analysis of the entire P-Sp/AGM population (top panels, boxes indicate windows used for sorting) and corresponding index sorting analysis (bottom panels), identifying each single cell with HSC potential (pre-HSC clone), hematopoietic colony formation without HSC potential (non-HSC hemogenic clone), or no hematopoietic colony formation (non-hemogenic clone) based on functional potential following AGM-EC co-culture. A) E11.5 AGM (corresponds to Figure 3A), B) E9.5 P-Sp (corresponds to Figure 3B, left panel), and C) E10.5 AGM (corresponds to Figure 3B, right panel).

Table S1. B cell engraftment from E9.5 and E11.5 pre-HSC clones, Related to Figures 1 and 2

Stage	# of Clones Analyzed	% Donor PB Engraftment Mean±SEM (range)	% Donor Peritoneal Engraftment Mean±SEM (range)	# of Clones with B-1a Engraftment	# of Clones with B-2 Engraftment	%B-1a Cells in Peritoneum[a]	%B-2 Cells in Peritoneum[a]
E9.5	6	40±15 (8.9-88)	55±10 (31-86)	6	6	28±8	42±8
E11.5	27	76±0.8 (10-91)	80±1.1 (18-92)	27	27	*7.5±0.9	*71±2

[a]%B-1a and B-2 calculated as percent of total donor-derived IgM positive B cells detected in peritoneal washes. Shown is mean ± SEM; *$p<0.001$, E9.5 vs E11.5 (unpaired student t-test). Data for E9.5 is pooled from 4 independent experiments and for E11.5 from 2 independent experiments.

Table S2. List of Antibodies

Antigen	Clone	Fluorochrome(s)	Source	Catalog No.
CD45	30-F11	FITC, APC	eBioscience	11-0451
CD41	eBioMWReg30	PE, APC, APC-eFluor780	eBioscience	12-0411
VE-Cadherin	11D4.1	AlexaFluor647, PE	BD Biosciences	562242
VE-Cadherin	eBioBV13	PE/Cy7	eBioscience	25-1441
c-kit	2B8	APC	BD Biosciences	553356
Sca-1	D7	APC, PE/Cy7	eBioscience	17-5981
F4/80	BM8	APC-eFluor780, PE	eBioscience	47-4801
Gr-1/Ly6-G	RB6-8C5	APC-eFluor780, PerCP	eBioscience	47-5931
CD19	ID3	APC, PE	BD Biosciences	550992
B220/CD45R	RA3-6B2	PerCP	BD Biosciences	561086
TER-119	TER-119	PE	eBioscience	12-5921
CD3	17A2	FITC, PE	BD Biosciences	555274
CD4	RM4-5	PE	BD Biosciences	553049
CD8	53-6.7	PerCP	BD Biosciences	553036
CD150	TC15-12F12.2	PerCP/Cy5.5	BioLegend	115922
CD48	HM48-1	PE/Cy7, PE	BioLegend	103424
Delta-like-4	HMD4-1	APC	Biolegend	130814
EPCR/CD201	eBio1560	PE, PerCP-eFluor710	eBioscience	12-2012
CD45.1/Ly5.1	A20	PE/Cy7, eFluor450	eBiosciences	25-0453
CD45.2/Ly5.2	104	APC-eFluor780, PE/Cy7	eBiosciences	47-0454
CD11b/Mac1	M1/70	FITC, APC-eFluor780	eBiosciences	11-0112
IgM	R6-60.2	PerCP-Cy5.5	BD Biosciences	562034
CD23	B3B4	APC	Invitrogen	MCD2305
CD5	53-7.3	PE	BD Biosciences	553023
AA4.1	AA4.1	FITC	eBiosciences	11-5892
CD21	7G6	PE	BD Biosciences	552957